

The Electron-scavenging Process in 3-Methylhexane Glass at 77 K Studied by ESR

Koichi OKA, Hideo YAMAZAKI, and Shoji SHIDA

Laboratory of Physical Chemistry, Tokyo Institute of Technology, Meguro-ku, Tokyo 152

(Received December 4, 1972)

The effect of various additives, *i.e.*, nitrous oxide, sulfur hexafluoride, methyl chloride, and sulfur dioxide, on the yield of the trapped electrons produced in the γ -irradiated 3-methylhexane (3MHX) glass at 77 K have been investigated by the ESR technique. The yields of the trapped electrons were reduced by the addition of all the solutes examined; the efficiency of electron scavenging was found to be in the order of $\text{SF}_6 > \text{CH}_3\text{Cl} > \text{N}_2\text{O} > \text{SO}_2$. The concentration dependence of the electron scavengers showed that the efficiency of the electron scavenging in the glassy state had values intermediate between those in the gas and liquid phases. The high efficiency observed in the glassy state suggests that the non-solvated electrons before being trapped move about rapidly in the glassy matrix as the form of quasi-free electrons. The ESR-power saturation of the trapped electrons was considerably reduced by the addition of N_2O ; a possible mechanism of the relaxation of the ESR is proposed.

The electron-scavenging process is one of the most important problems in radiation chemistry. To examine this problem, physical methods, such as optical absorption measurement by means of pulse radiolysis,¹⁾ ESR studies,^{2,3)} and luminescence measurement,⁴⁾ have been used as well as the chemical method of product analysis. A considerable number of experiments have been made on electron scavenging by chemical analysis in the gas^{5,6)} and the liquid phases;⁷⁻⁹⁾ however, there has been little work in the glassy state.¹⁰⁾ The main difficulties of the product analysis in the glassy state at low temperatures are the fact that the spatial distribution of solutes may be nonhomogeneous and the fact that the overall reactions are not isothermal. Therefore, the kinetic treatment based on the homogeneous distribution of reactants and on the isothermal condition is not applicable. The physical methods may still give some insight into this problem, though concerning the nature of the trapped electrons, the spatial distribution has been studied by photobleaching¹¹⁾ and by the microwave-power saturation of ESR.^{12,13)} The structure

of the trapped electrons has also been studied by means of pulse radiolysis^{1,14)} and by ESR.^{3,15)} However, little study has been done on the electrons before being trapped. These electrons should resemble those photo-released from the trapped states,¹⁶⁾ 'mobile electrons,' but they may be different in energy.

In the present work, ESR has been used to measure the trapped electrons in 3-methylhexane (3MHX) glass and to obtain information on the electrons before they were trapped by the scavenger technique. The energy of electron attachment has been said to be different in each electron scavenger¹⁷⁻²⁰⁾ in the gas phase, so that the electrons are scavenged even in the solid phase. The ESR technique is expected to be useful for testing the efficiency of electron attachment in the solid phase. The electron scavengers (N_2O , SF_6 and CH_3Cl) used in the present work are well known, but SO_2 is not usually used in the gas and the liquid phases. In the present work, N_2O , one of the most important electron scavengers, has been studied in detail.²¹⁾ The trapped electrons decreased upon the addition of N_2O to the hydrocarbon matrix and also changed in their nature; the ESR-power saturation of the trapped electrons was remarkably reduced by the addition of N_2O .

Experimental

Pure-grade 3MHX (Aldrich Chemical Co.) was purified by passing it through an activated silica gel column; it was degassed by the freeze-pump method and stored in sodium-potassium alloy for more than a day before use. The gaseous materials, SF_6 , CH_3Cl , N_2O and SO_2 (Matheson Co.) were

1) H. A. Gillis, N. W. Klassen, G. G. Teather, and K. H. Lokan, *Chem. Phys. Lett.*, **11**, 12, (1971); I. A. Taub and H. A. Gillis, *J. Amer. Chem. Soc.*, **91**, 6507 (1969); N. V. Klassen, H. A. Gillis, and G. G. Teather, Report of National Research Council of Canada, Division of Physics RXNR 2321 (1972).

2) D. R. Smith and J. J. Pieroni, *Can. J. Chem.*, **45**, 2723 (1967).

3) H. Yoshida and T. Higashimura, *ibid.*, **48**, 504 (1970).

4) K. Funabashi, C. Hebert, and J. L. Magee, *J. Phys. Chem.*, **75**, 3221 (1971); M. Magat, "Progress and Problems in Contemporary Radiation Chemistry," Prague, p. 423 (1971); A. C. Albrecht, *ibid.*, p. 331.

5) P. Ausloos, *Progs. React. Kinet.*, **5**, 113 (1969); W. J. Holtslander and G. R. Freeman, *J. Phys. Chem.*, **71**, 2562 (1967).

6) G. R. A. Johnson and J. M. Warman, *Trans. Faraday Soc.*, **61**, 1709 (1965).

7) G. Scholos and M. Simic, *Nature*, **202**, 895 (1964).

8) F. Williams, *J. Amer. Chem. Soc.*, **86**, 3954 (1964).

9) J. M. Warman, K.-D. Asmus, and R. H. Schuler, *Advan. Chem. Ser.*, **82**, 25 (1968).

10) T. Wakayama, T. Kimura, T. Miyazaki, K. Fueki, and Z. Kuri, *This Bulletin*, **42**, 266 (1969); T. Sawai, Y. Shinozaki, and G. Meshitsuka, *ibid.*, **45**, 984 (1972).

11) W. H. Hamill, "Radical Ions," Ed. by E. T. Kaiser and L. Kevan, Wiley-Interscience, New York, (1968) p. 321.

12) K. Tsuji and F. Williams, *Trans. Faraday Soc.*, **65**, 1718 (1969).

13) J. Zimbrick and L. Kevan, *J. Chem. Phys.*, **47**, 2364 (1967).

14) J. T. Richards and J. K. Thomas, *ibid.*, **53**, 218 (1970).

15) J. Lin, K. Tsuji and F. Williams, *J. Amer. Chem. Soc.*, **90**, 2766 (1968).

16) F. S. Dainton and G. A. Salmon, *Proc. Roy. Soc. Ser. A*, **285**, 319 (1965).

17) D. Rapp and D. D. Briglia, *J. Chem. Phys.*, **43**, 1480 (1965).

18) L. G. Christophorou and J. A. D. Stockdale, *ibid.*, **48**, 1956 (1968).

19) R. P. Blaunstein and L. G. Christophorou, *ibid.*, **49**, 1526 (1968).

20) D. A. Raelis and J. M. Goodibgs, *Can. J. Chem.*, **49**, 1571 (1971).

21) S. Sato, *This Bulletin*, **41**, 304 (1968).

commercially obtained and were used without purification.

In a mercury-free system, 3MHX was measured with a measuring capillary (2 mm i.d.), and the amounts of gaseous material added were determined by means of an oil manometer with a flask of a constant volume. The Ostwald absorption coefficients of various electron scavengers in liquid 3MHX at room temperature were used to determine the concentration of the solutes in 3MHX glass at 77 K. The samples were sealed in a Suprasil quartz ESR tube (3 and 5 mm, i.d.) and irradiated for 20 min–4 hr by ^{60}Co γ -rays at 77 K in the dark, at a dose rate of 0.8×10^6 r/hr. After the irradiation, the ESR spectra of the samples were immediately measured in the dark by means of a JEP-1 X-band ESR spectrometer with a field modulation of 100 kHz. A multimode microwave cavity was used to determine the signal intensity by referring to a standard sample. After the initial measurement, bleaching experiments were performed with infrared light (>1000 nm) from a tungsten lamp through two Toshiba glass filters (V-B46 and IR-RIA).

In the saturation study the microwave power of ESR was measured by means of a thermistor power meter in the range of 0.01–10 mW. The magnetic field, H_1 , of the microwaves in the cavity under the present operating conditions was given approximately by the following relationship: $H_1 = 2.0 \times 10^{-2} P^{1/2}$, where P is the microwave power in mW and where H_1 is that in gauss.²²⁾ The power saturation curve was measured in the $1\text{--}10^{-3}$ mW range by the use of multimode microwave cavity at the modulation frequency of 100 kHz. The ratio of the saturation factor, Z , was directly measured from the signal-intensity ratio of the sample to a DPPH crystal, because the signal of the DPPH crystal was not entirely saturated under the conditions of the measurement.

Results

The ESR spectrum of γ -irradiated 3MHX glass is shown in Fig. 1. The singlet spectrum at the center is due to the trapped electrons (e_t^-) and is photobleached by the irradiation of infrared light. The remaining

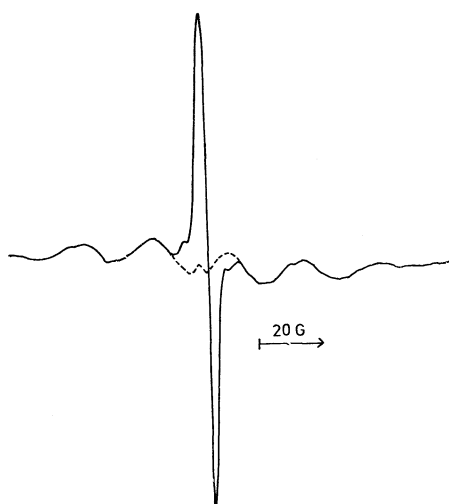


Fig. 1. ESR spectra of pure 3-methylhexane glass γ -irradiated to a dose of 9×10^{18} eV/g at 77 K. Solid curve; immediately after the irradiation, dotted curve; after the photobleaching by infrared light.

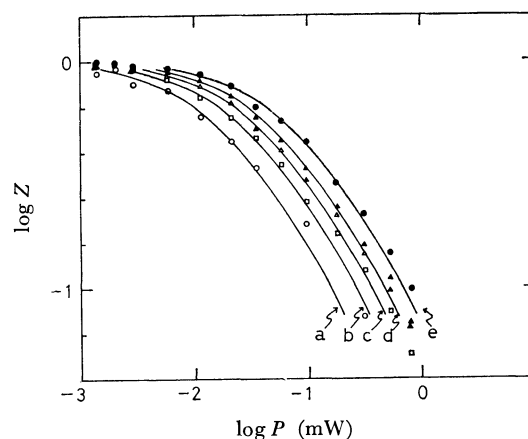


Fig. 2. Experimental values and theoretical curves of microwave-power saturation for e_t^- in 3-methylhexane glass at 77 K. The saturation factor, Z , is plotted as a function of microwave power, P , and the experimental values correspond to \circ ; 8.3×10^{18} , \square ; 17×10^{18} , \triangle ; 33×10^{18} , \blacktriangle ; 50×10^{18} , \bullet ; 10×10^{19} eV/g and the calculated curves correspond to a) $T_1 = 1.3 \times 10^{-2}$, b) 7.6×10^{-3} , c) 5.6×10^{-3} , d) 4.4×10^{-3} , e) 3.0×10^{-3} s.

spectrum is due to a free radical. The line shape of e_t^- is close to a gaussian. The line width of e_t^- between the maximum slope is about 3.5 ± 0.2 gauss and is broadened at a high microwave power. The singlet ESR spectrum of e_t^- was well resolved from that of the free radicals by photobleaching with infrared light. The microwave-power saturation of e_t^- was measured at various total doses. The experimental values coincide with the theoretical curves calculated by the saturation factor, as is shown in Fig. 2. With the irradiation doses between $(0.83\text{--}10) \times 10^{19}$ eV/g, the saturation curve moves gradually to the side of a high microwave power at high total dose, but the curvature does not change.

A study was made of the scavenging of e_t^- in γ -irradiated 3MHX glass at 77 K as a function of the electron-scavenger concentration. It is well known that the electron scavengers reduce the formation of e_t^- . The signal intensity of e_t^- decreased rapidly with the concentration of SF_6 (Fig. 3) and disappeared completely at a relatively low concentration compared with the cases of the other electron scavengers. The addition of SF_6 did not alter the line shape of the e_t^- signal and did not produce any new signal. The

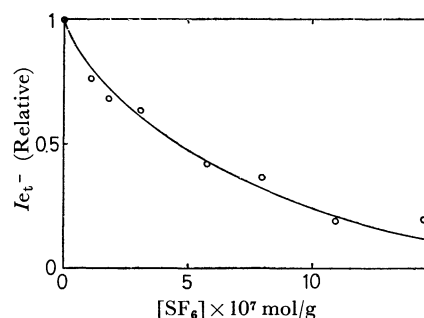


Fig. 3. Effect of addition of SF_6 on the relative signal intensity of e_t^- in 3-methylhexane glass at 77 K γ -irradiated to a dose of 2.0×10^{19} eV/g.

22) C. P. Poole, Jr., "Electron Spin Resonance," Interscience Publishers, New York (1967), p. 341.

microwave-power saturation curve of e_t^- shifted slightly to the side of the low power upon the addition of SF_6 .

When N_2O was added, the signal intensity of e_t^- decreased at the low microwave power. At a high microwave power, the signal intensity of e_t^- increased with the concentration of N_2O and then decreased, as is shown in Fig. 4. The line shape and the width of the e_t^- signal did not change upon the addition of N_2O , and the signal could be photobleached by the infrared light at any concentration of N_2O . However, when N_2O was added, the microwave-power saturation curve shifted to the side of the high power and the shape of the saturation curve changed, as is shown in Fig. 5.

Figure 6 shows the ESR spectrum of γ -irradiated 3MHX glass containing CH_3Cl . The signal at the center is due to e_t^- , and the quartet signal, to CH_3 . The microwave-power saturation curve of e_t^- did not shift upon the addition of CH_3Cl . After the photobleaching, the signal of e_t^- disappeared and that of

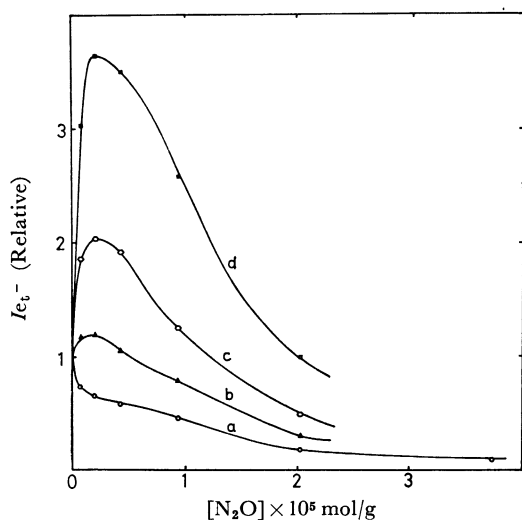


Fig. 4. Effect of addition of N_2O on the relative signal intensity of e_t^- for various microwave power in 3-methylhexane glass at 77 K γ -irradiated to a dose of 1.7×10^{19} eV/g: a) extrapolated value at the zero microwave power, b) 0.027 mW, c) 0.048 mW, d) 0.081 mW.

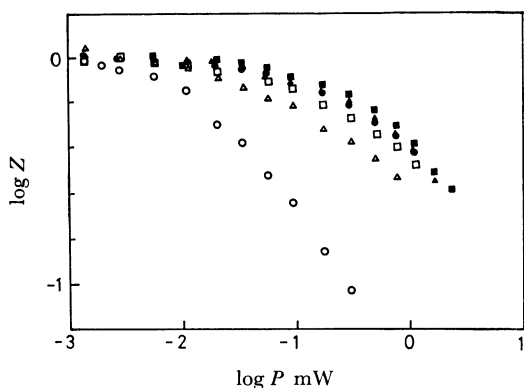


Fig. 5. Microwave-power saturation curve for e_t^- , plotting the saturation factor, Z , versus microwave power, P , in 3-methylhexane glass γ -irradiated to a dose of 1.7×10^{19} eV/g at 77 K: N_2O concentration of \circ ; 0×10^{-7} , \triangle ; 4.7×10^{-7} , \square ; 1.1×10^{-6} , \bullet ; 2.2×10^{-6} , \blacktriangle ; 4.7×10^{-6} , \blacksquare ; 10×10^{-6} mol/g.

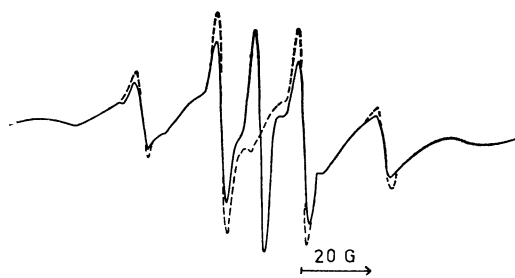


Fig. 6. ESR spectra of 3-methylhexane glass containing 3×10^{-6} mol/g CH_3Cl γ -irradiated to a dose of 9×10^{18} eV/g at 77 K. Solid curve; immediately after the irradiation, dotted curve; after the photobleaching by infrared light.

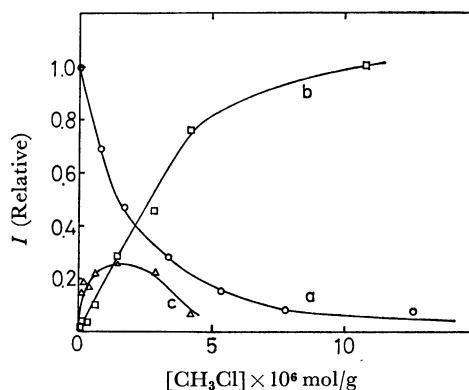


Fig. 7. Effect of addition of CH_3Cl on the relative signal intensity of e_t^- in 3-methylhexane glass γ -irradiated to a dose of 9×10^{18} eV/g at 77 K: a) e_t^- , b) CH_3 , c) the increment of CH_3 by photobleaching.

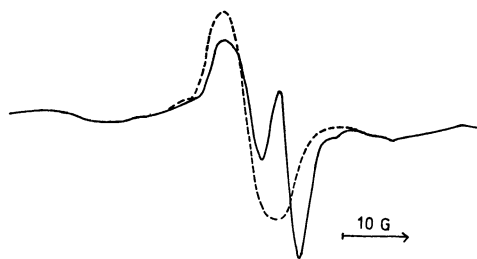


Fig. 8. ESR spectra of 3-methylhexane glass containing 5.4×10^{-6} mol/g SO_2 γ -irradiated to a dose of 9×10^{18} eV/g at 77 K. Solid curve; immediately after the irradiation, dotted curve; the photobleaching by infrared light.

CH_3 increased. As is shown in Fig. 7, the signal intensity of e_t^- decreased, while the quartet signal of CH_3 increased, with the concentration of $CHCl_3$, which underwent a dissociative electron attachment.

The ESR spectrum of γ -irradiated 3MHX glass containing SO_2 is shown in Fig. 8. A new singlet signal ($g=2.007$, $\Delta H_{msl}=8$ gauss) appeared in the presence of SO_2 , and the signal increased when the e_t^- was photobleached. The signal seems to be due to SO_2^- ; the ESR signal of SO_2^- formed from the adsorbed SO_2 on MgO has been measured by another method.²³⁾ The broad linewidth is probably due to the anisotropy of SO_2^- . Figure 9 shows that the signal

23) R. A. Schoonheydt and H. J. Lunsford, *J. Phys. Chem.*, **76**, 323 (1972).

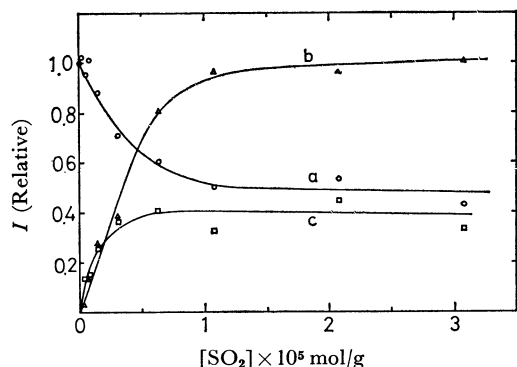


Fig. 9. Effect of addition of SO_2 on the relative signal intensity in 3-methylhexane glass γ -irradiated to a dose of $9 \times 10^{18} \text{ eV/g}$ at 77 K: a) e_t^- , b) SO_2^- , c) the increment of SO_2^- by photobleaching.

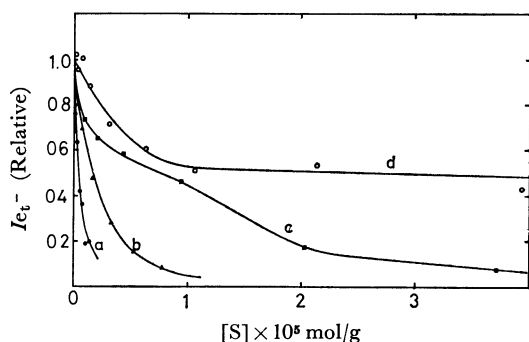


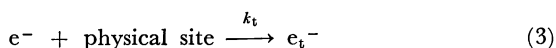
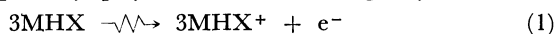
Fig. 10. Summary of the effect of addition of various electron scavenger on the relative signal intensity of e_t^- : a) SF_6 , b) CH_3Cl , c) N_2O , d) SO_2 .

intensity of e_t^- decreased, and that of SO_2^- increased, with the concentration of SO_2 . Even at high concentrations of SO_2 , the signal of e_t^- did not completely disappear.

The electron-scavenging studies of e_t^- in 3MHX by various electron scavengers are summarized in Fig. 10, which shows that the efficiency of electron scavenging obtained from the initial slope of the curves is in the order of $\text{SF}_6 > \text{CH}_3\text{Cl} > \text{N}_2\text{O} > \text{SO}_2$ and that the curvature of each scavenger is different from all others.

Discussion

In the absence of electron scavengers, the liberated electrons are either recombined with parent cations or trapped by physical sites in the glassy matrix:



where k_n and k_t are the rate constants of neutralization and of electron trapping. In the presence of the electron scavenger, S , a part of the electrons can be scavenged before the recombination or the trapping:



where k_s is the rate constant of electron scavenging. The measurement was made only of the decrease in the trapped-electron yield by the addition of the

scavengers in this experiment. The reaction of electron attachment competes with those of electron trapping and neutralization. If the reaction of the electron scavenging and the electron trapping are treated by homogeneous kinetics, the following equations are obtained:

$$G_0(e_t^-)/G(e_t^-) = 1 + (k_s/\tau)S \quad [1]$$

$$\tau = k_n[M^+] + k_t[\text{T.S.}] \quad [2]$$

where $G_0(e_t^-)$ is the G -value of e_t^- at zero scavenger concentration and where $[\text{T.S.}]$ is the concentration of the physical trapping site. Because the ion pairs neutralize geminately, the local concentration of parent cations, $[M^+]$, is a dose-independent constant in Eqs. [1] and [2], it is expressed microscopically as a function of the distance between the electrons and the parent cations. The concentration of the physical trapping sites was estimated to be larger than 10^{-3} mol/l from the total dosage effects.²⁴⁾ The relative rate constants of electron scavenging, k_s/τ , are obtained from the initial slope of the curves in Fig. 11, in which the plots for SF_6 and CH_3Cl are almost linear and in the curves for N_2O and SO_2 are concave downwards. The deviation of the plots from the straight line may be due to the fact that these reactions are not homogeneous. When k_s is very large, the concentration of scavengers can be relatively small in the measurement and the heterogeneity of the competition reaction may be ignored. The reciprocal concentration at which the yield of e_t^- decreases to a half, $1/S_{1/2}$, and the k_s/τ ratio are shown in Table 1. The values of k_s/τ and $1/S_{1/2}$ are the same sequences of series, and the $1/S_{1/2}$ ratio is almost ten times larger than k_s/τ . To express the efficiency of electron scavenging, the values of k_s/τ seem to be more adequate than that of $1/S_{1/2}$. The electron-scavenging efficiency of SF_6 in the liquid phase is found to be almost the same as that of N_2O by the measurement of the hydrogen depression,²⁵⁾ because the electrons were solvated and the efficiencies were determined by a diffusion-controlled process. In the gas phase, the ratio of efficiencies between SF_6 and

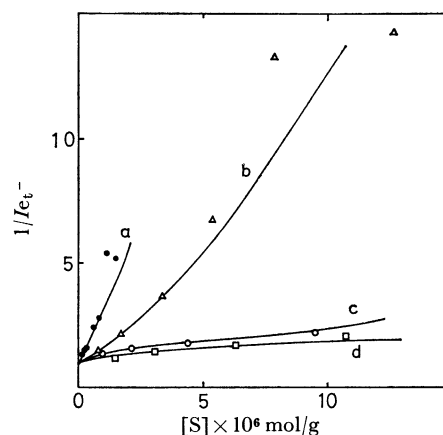


Fig. 11. The inverse of the relative signal intensity of e_t^- plotted versus the concentration of various electron scavenger: a) SF_6 , b) CH_3Cl , c) N_2O , d) SO_2 .

24) A. Ekstrom, R. Suenram, and J. E. Willard, *J. Phys. Chem.*, **74**, 1888 (1970).

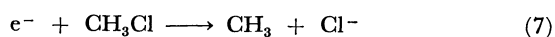
TABLE 1.

	Solid ^{a)}		Liquid $\alpha^{b)}$ l/mol	Gas		
	$1/S_{1/2}$ l/mol	k_s/τ l/mol		$1/S_{1/2}^{c)}$ l/mol	σ A ²	$\int \sigma(E)dE$ A ² eV
SF ₆	2×10^3	2×10^2	18	$\geq 3 \times 10^8$	2.15 ^{d)}	
CH ₃ Cl	6×10^2	6×10	(5)		0.058 ^{e)}	$1.54 \times 10^{-3} \text{ e)}$
N ₂ O	9×10	2×10	16	3×10^4	0.0978 ^{e)}	$1.05 \times 10^{-2} \text{ e)}$
SO ₂	—	10				

a) This work in 3MHX glass; b) From the measurement of hydrogen depression in liquid cyclohexane, α is equivalent to $1/S_{1/2}$ from Ref. 9; c) From the measurement of N₂ formation in gaseous propane by the addition of N₂O; d) Electron-attachment cross section by thermal electron from Ref. 17; e) Electron-attachment cross section by electrons of E_{\max} from Refs. 17 and 19.

N₂O was measured⁶⁾ and found to be about 10^4 and the electron-attachment cross sections were measured directly by the methods of mass spectrometry for negative ions,¹⁷⁻¹⁹⁾ as is shown in Table 1. The electron scavenging in the glassy state seems to have an intermediate character between those in the gas and liquid phases with respect to the ratios and the absolute values of $1/S_{1/2}$. These experimental results indicate that, before being trapped, the electrons interact with a solvent weaker than the solvated electrons in the liquid phase.

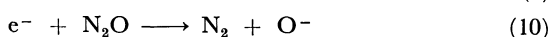
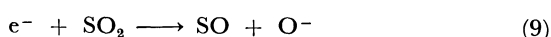
The formations of SO₂⁻ and CH₃ were observed by the use of ESR in the presence of SO₂ and CH₃Cl. The electron scavengers, SO₂ and CH₃Cl, attach to the electrons produced by γ -irradiation or by photobleaching of e_t⁻, and the negative ions or the free radicals appear by means of those reactions:



On the other hand, the electron scavenging by SF₆ and N₂O produces no negative ions or free radicals. The solute, SF₆, attaches to the electrons as intermediate species:



The pair of SF₆⁻ and the parent cation is unstable and is neutralized by electron jumps from the negative ions or by the migration of negative ions in the matrix. In the CH₃Cl solution, however, the dissociative electron attachment by CH₃Cl takes place,²⁶⁾ and an ion pair of Cl⁻ and the parent cations forms near the CH₃ radicals by means of the cage effect of a glassy matrix. The ion pair must be unstable and must be neutralized to leave CH₃ radicals. In the experimental results of low-pressure mass spectrometry, SO₂ and N₂O attach dissociatively to electrons with some energy by the formation of O⁻:



The cage effect in glassy matrix disturbs the dissociative

electron attachment of SO₂, and SO₂⁻ is formed. However, N₂O⁻ dissociates easily, and the parent cations are neutralized by O⁻ migration in the matrix. Therefore, no negative ion were trapped in the matrix by the addition of N₂O.

The energy distribution of electrons, $p(E, t)$, is the function of the electron energy, E , and the time, t . When the electrons are thermalized, the spatial distribution, $D(r)$, is the integrated product of the degradation factor, $R(E, r)$, and the initial energy distribution, $\int R(E, r)p(E, 0)dE$, where r is the distance between electrons and the parent cations. If the electrons are trapped after a complete thermalization and if the concentration of trapping sites is very large, the portion of ionic species being trapped is the integrated product, $4\pi \int r^2 D(r)\phi(r/r_t)dr$,²⁷⁾ where $\phi(r/r_t)$ is the probability of electron trapping, where r_t is $e^2/\epsilon V_t$, where ϵ is the dielectric constant, and where V_t is the depth of the physical or chemical site. When r is larger than r_t , $\phi(r/r_t)$ can be expected to be large. The chemical site is usually deeper than the physical site. When the concentration of electron scavengers is small, the electron-scavenging efficiency, k_s , is proportional to the integrated cross section of electron attachment, $\int \sigma(E)P(E)Q(E)dE$, where $\sigma(E)$ is the cross section of electron-scavenging as a function of the electron energy, $p(E) = \int p(E, t)dt$ is the time-average distribution of electrons, and $Q(E)$ are the portions of electrons which should have been physically trapped in the absence of the electron scavengers. In a glassy matrix, $Q(E)$ will be small for the electrons near the thermal energy, because the electrons in the low-energy population will geminately recombine with the parent cation and will not contribute to the reaction with the scavengers. Therefore, $P(E)Q(E)$ in the glassy state will more likely be the energy distribution function in the gas phase than that in the liquid phase, where the collisional deactivation is easier than in the glassy state, so that energy is distributed only

25) P. P. Infelta and R. H. Schuler, *ibid.*, **76**, 987 (1972).

26) "Fundamental Processes in Radiation Chemistry," Ed. by J. E. Willard and P. Ausloos, New York, Interscience Publishers (1968), p. 620.

27) If the function, $\phi(r/r_t)$, is similar to Onsager's equation, Laplace transformation of yield of trapped species as a function of various scavengers, r_t , will be obtained as the function, $D(r)$. Assumption of Magee's process, other functions $P(E)$ and $p(E, t)$, can be written as function of $D(r)$.

near the thermal energy in the liquid phase. In the electron-scavenging process, it is important to know what percentage of the total ionization is trapped. By the ESR and photoabsorption methods, the G -value of electron trapping, $G(e_t^-)$, in 3MHX glass at 77 K is 0.9.¹⁵⁾ In the gas phase, however, the yield of ionization has been estimated from the W -value²⁸⁾ to be 4. If the ionization efficiency is the same in the gas and solid phases, the portion of electrons being trapped in the 3MHX glass, $\int P(E)Q(E)dE = 4\pi \int r^2 D(r)(r/r_t)dr$, is estimated to be 0.2 ($\approx 0.9/4$).

Recently, however, the quasi-free electron model²⁹⁾ has successfully been applied to the behavior of electrons in the condensed phase, so the electron-scavenging process should be reexamined from this point of view. In the gas phase, the cross section of electron attachment with scavengers has been measured as a function of the electron energy. For example, the electron energies for the maximum cross section, E_{\max} , of SF_6 , N_2O , and CH_3Cl are, respectively, 0.02,¹⁷⁾ 2.25,¹⁸⁾ and 0.02 eV,¹⁹⁾ while the E_{\max} of SO_2 has two values, 5 and 8 eV.²⁰⁾ When E_{\max} is small, for example, in the cases of SF_6 and CH_3Cl , k_s is reduced to being proportional to $\int \sigma(E)dE$, considering that $P(E)Q(E)$ is constant in the range of near-thermal energies, in contrast with the rapid change of $\sigma(E)$ in this region. Even at high concentrations, SO_2 can not scavenge a part of the electrons, because the $\sigma(E)$ of SO_2 is nearly zero at a small electron energy.

The saturation study of ESR also provides information on the structure of e_t^- . The rapid and fast passage and the nonadiabatic condition ($H_1/H_m\omega_m \ll \sqrt{T_1T_2}$, $\omega_m T_1 \gg 1$, $\gamma H_1^2 \ll \omega_m H_m$)³⁰⁾ are given by the data of Tsuji and Williams¹²⁾; T_1 is about 10^{-2} – 10^{-3} , T_2 is about 10^{-7} – 10^{-8} , $\sqrt{T_1T_2}$ is about 10^{-5} – 10^{-6} , the angular frequency of magnetic-field modulation, ω_m , is $2\pi \times 10^5$, and the peak modulating magnetic field, H_m , is about 1 gauss in this experiment, where H_1 is the component of the rotating magnetic field, perpendicular to the z -direction and where γ is the gyro-magnetic ratio. The spin-lattice relaxation time, T_1 , given by the equation of the saturation factor, $Z = (1 + 2\gamma H_1^2 T_1 / \pi H_m)^{-1}$,³⁰⁾ is not accurate because of the error in H_1 values, but the relative values give useful information regarding the structure. The higher microwave-power saturation curve of e_t^- in pure 3MHX (Fig. 2) agrees with the equation of Z , and shift to a microwave power shows the decrease in T_1 with an increase in the total dose. However, the shift to the higher microwave power in Fig. 5 shows the decrease in T_1 with the concentration of N_2O . In addition to the shift, the shape of the saturation curve changes when N_2O is added. Because the variation in T_1 and T_2 values due to the addition of N_2O affects the

conditions of the power-saturation measurement, a different type of equation for the saturation factor should be applied. The singlet signal of the trapped electrons produced by the addition of N_2O is different from that in pure 3MHX glass and has the following properties: 1) the signal has the same ESR linewidth at any concentration of N_2O and is photobleached by the infrared light much like the trapped electrons in pure 3MHX glass; 2) the signal disappears at a large concentration of N_2O ; 3) in the presence of N_2O , the absorption spectrum shows a broad near-infrared band which shifts to a slightly shorter wavelength than that in pure 3MHX³¹⁾; 4) no such shift of the absorption band or change in the ESR relaxation time can be observed in a polar matrix such as 2-methyl-tetrahydrofuran.³¹⁾ These phenomena must result from the formation of trapped electrons in a slightly different structure, and must not be due to negative species such as N_2O^- .

The spin-lattice relaxation mechanism is partly due to the spin-orbit coupling of the Van Vleck theory,³²⁾ partly to the modulation of the spin-spin interaction by the lattice vibrations (Waller theory),³³⁾ and partly to the cross relaxation by the spin-spin interaction.³⁴⁾ The transition due to the spin-orbital interaction of the trapped electrons in pure 3MHX must be small; it has the same value for any sample, no matter the total dose, but the geometrical change in the structure of the trapping site should affect this value. When N_2O is added, the electrons may be trapped near the N_2O molecule and the field in the trapping sites appears to be perturbed by N_2O , so that the spin-orbit interaction increases. However, the spin-spin interaction is related to the overlapped area of the ESR spectra; therefore, the interaction of the $e_t^- - e_t^-$ type is greater than that of the $e_t^- - R$ (free radical) type. In the Waller mechanism, the $e_t^- - e_t^-$ interaction may dominate the $e_t^- - R$ interaction. The cross relaxation depends on the facts that the spins of R are in good contact with the lattice and that those of e_t^- are in poor contact. Therefore, the cross relaxation takes place via the spin-lattice relaxation of R by the mutual spin flip between e_t^- and R . At any rate, the spin-lattice relaxation increases with an increase in the concentrations of the spins due to the e^- and free radicals, whose concentrations are related to the total doses of irradiation. The addition of SF_6 decreases the concentrations of e_t^- and free radicals, and the rate of spin-lattice relaxation is decreased. When CH_3Cl is added, the concentration of e_t^- decreases and that of CH_3 increases, so that the decrease in the spin-lattice relaxation by the Waller mechanism of the $(e_t^- - e_t^-)$ type will be partially compensated for by the increase in that of the $(e_t^- - R)$ type caused by the cross relaxation. Therefore, the total amounts of spin-lattice interaction seem to be almost the same.

31) Private communication from S. Sato; and S. Mizutani, Tokyo Institute of Technology Thesis for master's degree (1971).

32) J. H. Van Vleck, *J. Chem. Phys.*, **7**, 72 (1939).

33) I. Waller, *Z. Physik*, **79**, 370 (1932); J. H. Van Vleck, *Phys. Rev.*, **57**, 426 (1940).

34) N. Bloembergen, S. Shapiro, P. S. Pershan, and J. O. Artman, *ibid.*, **114**, 445 (1959).

28) P. Alder and H. K. Bothe, *Z. Naturforsch.*, **20** a, 1700 (1965).

29) K. Fueki, D. -F. Feng, and L. Kevan, *Chem. Phys. Lett.*, **13**, 616 (1972); H. T. Davis, L. D. Schmidt and R. M. Minday, *ibid.*, **13**, 413 (1972).

30) M. Weger, *Bell. System Tech. J.*, **39**, 1013 (1960).